



SPE 77427

Geostatistical Assignment of Reservoir Properties on Unstructured Grids

C. V. Deutsch, SPE, University of Alberta, T. T. Tran, SPE, ChevronTexaco and
M. J. Pyrcz, University of Alberta

Copyright 2002, Society of Petroleum Engineers Inc.

This paper was prepared for presentation at the SPE Annual Technical Conference and Exhibition held in San Antonio, Texas, 29 September–2 October 2002.

This paper was selected for presentation by an SPE Program Committee following review of information contained in an abstract submitted by the author(s). Contents of the paper, as presented, have not been reviewed by the Society of Petroleum Engineers and are subject to correction by the author(s). The material, as presented, does not necessarily reflect any position of the Society of Petroleum Engineers, its officers, or members. Papers presented at SPE meetings are subject to publication review by Editorial Committees of the Society of Petroleum Engineers. Electronic reproduction, distribution, or storage of any part of this paper for commercial purposes without the written consent of the Society of Petroleum Engineers is prohibited. Permission to reproduce in print is restricted to an abstract of not more than 300 words; illustrations may not be copied. The abstract must contain conspicuous acknowledgment of where and by whom the paper was presented. Write Librarian, SPE, P.O. Box 833836, Richardson, TX 75083-3836, U.S.A., fax 01-972-952-9435.

Abstract

Reservoir simulation is often performed on irregular non-Cartesian grids. A common methodology for building the input reservoir models is to perform geostatistical reservoir models on a fine grid and then to average them to the coarser unstructured grid. This method is computationally expensive; a more efficient approach is to modify the geostatistical algorithms to directly populate the unstructured grid.

The required modifications are described in this paper. First, direct simulation must be used in place of the more common Gaussian simulation. This is required because reservoir properties do not average linearly after Gaussian transformation; averaging is required because each grid block potentially has a different volume. Second, volume averaged variogram or covariance values are required between two arbitrary blocks $v_1(\mathbf{u})$ and $v_2(\mathbf{u}')$. These must be calculated quickly and efficiently. Third, to maintain a reasonable speed of geostatistical simulation on unstructured grids a customized search and a non-stationary covariance lookup table of the average covariance between blocks is required. Finally, directional permeability requires a special transformation to account for the nature of averaging.

We present the implementation details and some results using tartan and radial grids.

Introduction

Unstructured grids may not be Cartesian and the grid blocks may have different volumes; however, irregular grids defined by local grid refinement, corner point grids, Voronoi grids and so on are all called unstructured grids.

Geostatistical simulation algorithms are commonly applied to populate a regular grid of locations where the locations

being simulated are all at the same volume scale as the data used for simulation. The irregularity of the locations being simulated could be handled by simply modifying the search for previously simulated grid nodes. The problem with unstructured grids is the volume difference between different grid blocks.

Geostatistical prediction of grid blocks using data at much smaller scale and nearby grid blocks of different size is possible using the volume average of the covariance or variogram function. The average covariance is classically defined as:

$$\bar{C}(v_1, v_2) = \frac{1}{|v_1| |v_2|} \iint_{v_1 v_2} C(u - u') du du' \quad (1)$$

This is approximated very well by a numerical integration where 10 or more locations discretize each volume.

Block cokriging with average covariance values between each of the (block) data and between the data and the block being estimated is well established as a means of integrating different data types at different scale. Classical geostatistical references give all needed details^{1,2}. This formalism amounts to assuming that the variable under consideration averages linearly. Our main concern is that data do not average linearly after Gaussian transformation. For example, averaging equally representative volumes of 1% porosity and 40% porosity. The correct average is 20.5% because porosity averages arithmetically. If the porosity histogram is lognormal, the back transformed average would be 6.3%, which is significantly biased. For this reason, direct simulation must be used for geostatistical assignment of reservoir properties on unstructured grids.

Two issues have slowed the widespread adoption of direct sequential simulation (DSS) for geostatistical simulation: (1) reproduction of the global histogram within reasonable statistical fluctuations, and (2) accounting for the proportional effect (higher variability in high valued areas) in the simulation. Solutions to these problems are described herein.

Sequential simulation requires that nearby data and previously simulated grid blocks be used in kriging. The path in sequential simulation is random to avoid artifacts. The typical spiral search of sequential simulation must be modified to account for the unstructured grid. Two alternatives are presented: (1) spiral search according to a non-stationary

covariance lookup table, and (2) a super block search using the centroid locations of the grid blocks.

DSS does not solve the problem for permeability since it does not average linearly. The permeability tensor depends on the variability at all smaller scales and on the flow boundary conditions. We propose the use of power law averaging to transform the directional permeability to a variable that averages linearly³. DSS is applied on the power law transformation and the result is back transformed. The directional permeability values are different because the averaging depends on direction and yet the directional permeabilities are clearly related. A mathematical relationship is developed. Cosimulation is an alternative.

Methodology I: Direct Sequential Simulation

The key idea of direct sequential simulation (DSS) methodology has been available for many years⁴. Proceeding in a sequential path and drawing the simulated value from a distribution with a mean and variance given by cokriging will ensure that the variogram is reproduced. Variety of different volume supports can be used. The mean or kriging estimate can be written for any type and volume data:

$$y_{v_0}^*(\mathbf{u}) = \sum_{i=1}^n \lambda_i \cdot y_{v_i}^{t_i}(\mathbf{u}_i) \quad (2)$$

By convention, the estimate $y_{v_0}^*(\mathbf{u})$ is for variable type one representing volume v_0 , the n data are given weights λ_i , $i=1, \dots, n$, each data $y_{v_i}^{t_i}(\mathbf{u}_i)$ could be of a different type t_i and different volume support v_i . The well-known simple cokriging equations are used to calculate the weights:

$$\sum_{j=1}^n \bar{C}_{t_j, t_i}(v(\mathbf{u}_j), v(\mathbf{u}_i)) = \bar{C}_{1, t_i}(v(\mathbf{u}_0), v(\mathbf{u}_i)), \quad i=1, \dots, n \quad (3)$$

The average (cross) covariance is defined in equation 1 and is discussed in more detail below. The kriging variance is commonly used as the variance of the local distribution of uncertainty:

$$\sigma_K^2 = \bar{C}_{1,1}(v(\mathbf{u}_0), v(\mathbf{u}_0)) - \sum_{i=1}^n \lambda_i \cdot \bar{C}_{1, t_i}(v(\mathbf{u}_0), v(\mathbf{u}_i)) \quad (4)$$

The kriging variance assumes homoscedasticity, that is, the variability does not depend on the local mean; however, real variables systematically show heteroscedasticity or specifically the proportional effect. Figures 1 and 2 show how data in original units systematically show a proportional effect. These figures also show that the proportional effect is largely removed by a univariate Gaussian (normal scores) transformation. This justifies the common practice of sequential Gaussian simulation assuming that there is no proportional effect, that is, homoscedasticity. Many data sets were checked with the same results: real data shows a proportional effect and that effect is essentially removed after normal score transformation.

We suggest that the DSS procedure (1) use a standardized variogram in kriging, (2) calculate the standardized kriging

variance $\sigma_K^2(u)$, and (3) the rescale that variance to a local measure of variability $\sigma_{QS}^2(u)$ by:

$$\sigma_{QS}^2 = f(m^*(\mathbf{u}_0)) \cdot \sigma_K^2 \quad (5)$$

This requires two additional steps (1) fitting the proportional effect $f(m)$, and (2) calculating the local mean at each location $m^*(u)$. The proportional effect can be fitted with regression from plots like those shown in Figures 1 and 2. The local mean can be calculated by a number of methods: kriging with a large search radius or moving window averages.

The local distributions in DSS are parameterized by a mean (see Equation 2) and variance (see Equation 5). The shape of each conditional distribution must also be determined. A framework for the first requirement has been presented by Tran et. al⁵. A series of distributions, parameterized by estimate and variance that result in the global distribution being honored are constructed. This procedure utilizes the link between the global direct distribution and the Gaussian distribution. The simulated value z^s for quantile q is written:

$$z^s = F^{-1}[G_{\{0,1\}}^{-1}[G_{\{m,\sigma\}}^{-1}(q)]] \quad (6)$$

where m and σ are the mean and standard deviation of the local distribution.

It has been demonstrated by Oz et. al⁶, that the above quantile transformations may be avoided by characterizing the Z distribution with Hermite polynomials.

Regardless of the procedure applied to calculate the valid local distributions, there is a need to avoid repetitive calculations of the Z space quantiles. For example, given 100 quantiles are required to characterize the local distributions and 1,000,000 nodes in the model, this results in 100,000,000 quantile calculations for each realization.

Repetitive calculations are avoided by building a local distribution look up table. A range of means and variances of the standard normal distribution is discretized and the resulting Z space local distributions are calculated. The means and variances of these new distributions are calculated and the distributions are stored in a look up table. To speed up table retrieval a super block search is applied. An example local distribution look up table is illustrated in Figure 3.

These two important recent developments (the use of a quasi-stationary variance and the local distribution shape determination) have made the well known DSS approach suitable for practical application.

Methodology II: Average Covariances

The common approach to calculate the mean covariance (refer back to equation 1) between two volumes (v_1 and v_2) is to discretize the volumes and average the point covariance over all combinations of discretized nodes between v_1 and v_2 .

$$\bar{C}(v_1, v_2) \cong \frac{1}{n \cdot n'} \sum_{i=1}^n \sum_{j=1}^{n'} C(u_i - u_j) \quad (7)$$

An acceptable number of discretizations in 3-D is 4 in each direction⁷. An average covariance calculation requires $4^6 =$

16,384 calculations. Steps have to be taken to keep CPU time under control.

One way to speed up the covariance calculation is to build a covariance look up table that corresponds to each variogram. This replaces the variogram calculation with an index calculation. This lookup table must have sufficient detail to avoid numerical errors in subsequent calculations; no problems have been found when 100s of points are used.

Methodology III: Search/Covariance Lookup Table

A nonstationary average covariance table is built to further reduce redundant calculations. The average covariance between all volumes that are closer than the variogram range are calculated and stored. Then, during DSS, the covariances needed for kriging are read directly from this table.

The covariance table includes all possible combinations of average covariances between volumes, $\bar{C}(v_i, v_j)$. This results in redundancy in the nonstationary average covariance table since $\bar{C}(v_i, v_j) = \bar{C}(v_j, v_i)$, but greatly simplifies the look up of average covariance values. This redundancy allows the covariance table to be divided into separate subsets with all the required covariances associated with a specific volume in a subset. Fast lookup is accomplished with a pointer array that indicates the location of each subset within the covariance table.

In addition the nonstationary covariance table is sorted in the order of increasing covariance within each subset. This allows the nonstationary covariance table to be used directly in the search. The relevant grid blocks at a particular location are identified from the covariance table. The closest grid blocks can be checked first until a sufficient number are found.

Given a positive definite covariance model and correctly calculated mean covariances the kriging variance is non-negative. Nevertheless, when simulating irregular volumes, screening can cause extreme positive and negative kriging weights. See Figure 4 for example configurations that result in extreme weights. This is true regardless of the precision with which the average covariance values are calculated. Such extreme weights are rare when simulating directly to a regular grid. These extreme weights will cause the kriged estimate to be unusually large or small. These extreme weights may be dealt with by (1) modifying search to remove the data that are excessively screened, by (2) iteratively solving the kriging matrix or by (3) applying an octant search to reduce the potential of screening.

In the first method the unusual weights are eliminated by rejecting any conditioning data or previously simulated blocks that are “shadowed” by a closer data (see Figure 5). This is accomplished by creating a Boolean matrix representing the nodes within the range of correlation of the location being estimated. When a datum is selected to condition this unknown location (at the center of the Boolean matrix) a shadow template is positioned with the apex on the datum.

All locations within this template are set to ‘false’ and may not be subsequently selected as conditioning data for this estimate.

In the second method the search is performed in the usual fashion and kriging matrix is solved. Then the weights are checked, and if any weights are extreme, $|\lambda_i| \geq \text{threshold}$, then the corresponding data is removed and the kriging matrix a solved again. This method has the advantage of applying the correction only when required and should not significantly increase CPU time since cases with extreme weights are generally infrequent.

In the third method the number of data gathered from each octant is limited. Limiting the conditioning from each octant reduces the opportunity for screening.

Methodology IV: Permeability Averaging

Implicit to linear estimation (equation 2) and integration for average covariance values (equation 1) is the assumption of arithmetic averaging, that is, the variable averages linearly. Direct simulation removes the requirement for Gaussian transformation, which has been a historic problem; however, the problem remains for permeability.

Power law averaging effectively transforms the directional permeability to a variable that averages linearly. The general formula for power law averaging of the continuous variable K is written:

$$K_{eff} = \left[\frac{1}{v} \int k(\mathbf{u})^\omega d\mathbf{u} \right]^{\frac{1}{\omega}} \quad (8)$$

v is the volume over which the average is calculated, $k(\mathbf{u})$ is the permeability at location \mathbf{u} within the volume, and ω is an exponent of averaging. The effective permeability, K_{eff} , of a 3-D network of blocks must take a value between the harmonic and arithmetic average of the constituent permeabilities, depending on their spatial arrangement. The lower-bound harmonic average can be seen as a power average with $\omega = -1$; this is representative of flowing through a series of alternating permeability layers. The upper-bound arithmetic average can be seen as a power average with $\omega = +1$; this represents parallel flow through alternating permeability layers. The geometric average is obtained at the limit when $\omega = 0$.

The averaging power for each geologic setting must be calibrated. The calibration process for a single geological model is straightforward. The numerical model of small-scale permeabilities is subjected to flow simulation with specified boundary conditions to obtain the true effective permeabilities: K_x , K_y , and K_z . The directional averaging exponents, ω_x , and ω_y and ω_z , are chosen such that the power-law average matches the flow simulation results.

To account for uncertainty and fluctuations in the geological models, the calibration process is repeated for multiple realizations of the same geological model. Once an assemblage of directional ω values have been calculated, the resulting distributions can be checked. The mean value will

provide a single estimate for ω in a given direction, and the distribution will show the uncertainty in ω for the geological model^{3,8,9}.

DSS is applied on the power law transformation of variables that do not average linearly and the result is back transformed.

Application to Tartan Grids

The previous sections have discussed all of the methods required to apply DSS. They could be used/applied to any unstructured grid. A program called TARTANSIM has been assembled from the SGSIM program from GSLIB¹⁰ for demonstration. This program allows the “dx” and “dy” values to be specified as arrays instead of as constant values. The correct average covariances are calculated and other implementation details are considered.

As a first example, unconditional simulations generated by SGSIM and TARTANSIM were compared (see Figures 6 and 7). The SGSIM realizations were simulated on a 100 x 100 grid and then block averaged to a 15 x 15 tartan grid. The variogram was set as a single isotropic spherical structure with a range equal to 1/5 of the size of the model. The e-type estimates over 201 realizations were compared; they were identical, which indicates that TARTANSIM results are unbiased. Local distributions of uncertainty were also validated. Finally, the covariance between adjacent blocks was checked. The actual mean covariance calculated with the variogram model was compared to the covariance between adjacent blocks over 201 realizations. The covariance values are reproduced.

The GSLIB data set was then used as conditioning data. See Figure 8 for the location map. 201 realizations were generated with SGSIM with a 100 x 100 resolution. These realizations were block averaged to a tartan grid (see 9 for some example realizations). The same conditioning data were applied to TARTANSIM and the simulation was performed directly to the tartan grid (see Figure 10 for some example realizations).

The e-type estimate was calculated over the 201 realizations for both TARTANSIM and block averaged SGSIM results (see Figure 11). The e-type maps indicate that the conditional means from TARTANSIM are similar to the theoretically established SGSIM results. Some example local distributions of uncertainty were compared and the covariance between adjacent blocks was once again checked. The covariance from the realizations is less than the model covariance (in both SGSIM and TARTANSIM) because of the conditioning data. The results are correct.

A module is included with TARTANSIM for the simulation of nested radial grids. The radial grids are simulated after the tartan grid. The method for simulation of the radial grid is similar to that of TARTANSIM. An adapted nonstationary covariance table and a matrix building subroutine are used. Since all the mean covariances are precalculated and stored in a 2D matrix the search and construction of the kriging matrices is very rapid. An example

with the previous conditioned data set and 6 nested radial grids is shown in Figure 12. Figure 13 zooms in one of the radial grids.

Limitations

The methods presented in this paper make it feasible to directly populate unstructured grids with geostatistical techniques. There are, however, a number of limitations.

The first limitation is consideration of geological rock types. Assigning a discrete categorical rock type to relatively small geological modeling cells is reasonable; large grid blocks, however, are almost certainly a mixture of different rock types. This makes it awkward to condition the assignment of porosity and permeability.

Another limitation is the inability to use conventional validation techniques on the simulated realizations. Common practice when simulating to regular grids is to validate the results by checking the resulting distributions and spatial correlation (the variogram) of the realizations. There are a variety of checks that may be performed with realizations based on unstructured grids.

The dispersion variance may be checked by calculating the variance of similar sized blocks, v . Then this dispersion variance may be compared with the dispersion variance predicted by the variogram.

$$D^2(v, V) = \bar{\gamma}(V, V) - \bar{\gamma}(v, v) = \bar{C}(v, v) - \bar{C}(V, V) \quad (9)$$

Also, the average covariance may be calculated between blocks with multiple realizations.

$$\bar{C}(v_1, v_2) \cong E\{Z_{v_1} \cdot Z_{v_2}\} - E\{Z_{v_1}\} \cdot E\{Z_{v_2}\} \quad (10)$$

This experimental block to block covariance may be compared with the predicted from the variogram (see equation 7).

Conclusions

The major implementation obstacles to DSS, (1) reproduction of the global histogram within reasonable statistical fluctuations, and (2) accounting for the proportional effect (higher variability in high valued areas) in the simulation, have been discussed and solutions have been presented.

Key implementation details for the direct simulation to unstructured grids have been documented in this work. These methods describe the efficient calculation of (1) valid Z space distributions of uncertainty for all possible kriging estimates and estimation variances and (2) mean covariances for unstructured grids based on rectangular parallelepipeds.

Search issues which result in anomalous weights, out of place local realizations, and negative variances have been discussed and demonstrated. Three techniques, template screening of conditioning data, iteration of the kriging solution and octant search have been introduced.

The method of applying power law averaging to variables that do not average linearly has been discussed. This forward

transform results in a linear averaging variable that may be simulated directly and then back transformed a posteriori.

DSS to unstructured grids has been demonstrated through an example program TARTANSIM. A tartan grid was simulated with DSS the results validated by comparison to block averaged SGSIM results.

Acknowledgements

We are grateful to the industry sponsors of the Centre for Computational Geostatistics at the University of Alberta and to NSERC and ICORE for supporting this research.

References

1. Deutsch, C.V. and Journel A.G. (1998). *GSLIB: Geostatistical Software Library: and User's Guide*, Oxford University Press, New York, 2nd Ed., P92
2. Journel, A.G. and Huijbregts, Ch.J. (1978). *Mining Geostatistics*, Academic Press, New York. P304
3. Journel, A.G, Deutsch, C.V., Desbarat, A., "Power averaging for block effective permeability," SPE paper 15128, 1986.
4. Journel, A.G., Class notes on sequential simulation, Stanford University, CA, 1986
5. Tran, T.T., Deutsch, C.V., and Xie, Y., "Direct geostatistical simulation with multiscale well, seismic, and production data", SPE Annual Technical Conference and Exhibition, New Orleans, September 30 – October 3, 2001, SPE# 71323
6. Oz, B., Ortiz, J.C., Deutsch, C.V., "Determining the Shape of Conditional Distributions with Hermite Polynomials and Disjunctive Kriging" CCG 4th Annual Report, 2002.
7. Journel, A.G. and Huijbregts, Ch.J. (1978). *Mining Geostatistics*, Academic Press, New York. P97
8. Desbarats, A.J. "Numerical estimation of effective permeability in sand-shale formations," Water Resources Research, 23; 2, P273-286, 1987.
9. Deutsch, C.V. "Calculating effective absolute permeability in sandstone/shale sequences," SPE Formation Evaluation, September 1989.
10. Deutsch, C.V. and Journel A.G. (1998). *GSLIB: Geostatistical Software Library: and User's Guide*, Oxford University Press, New York, 2nd Ed., P170

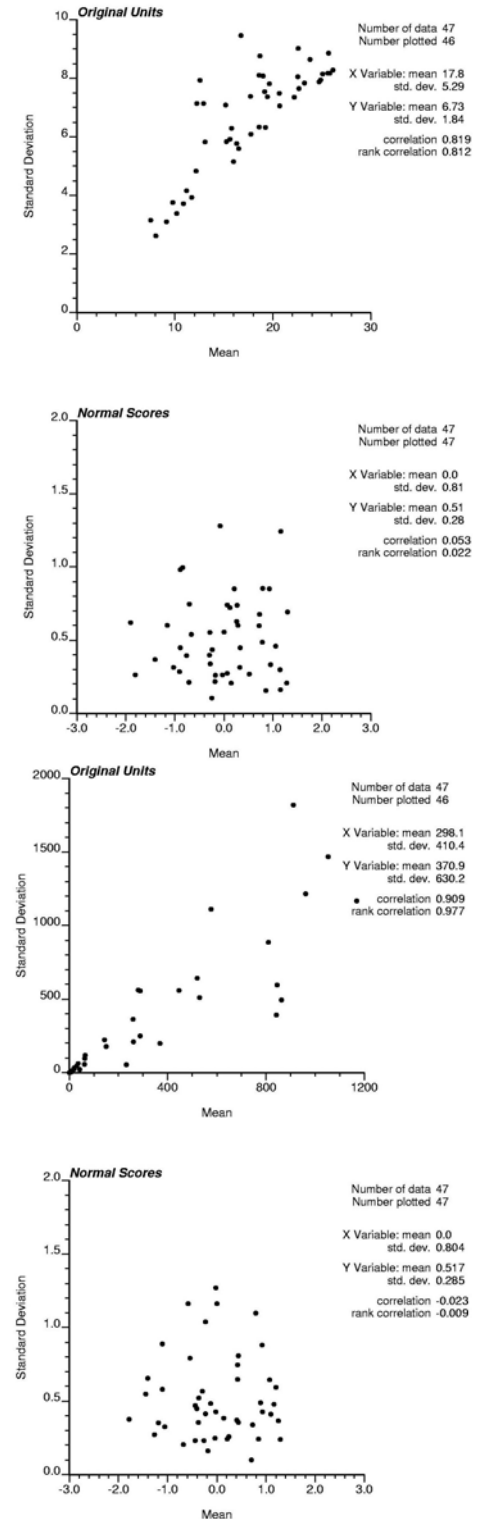
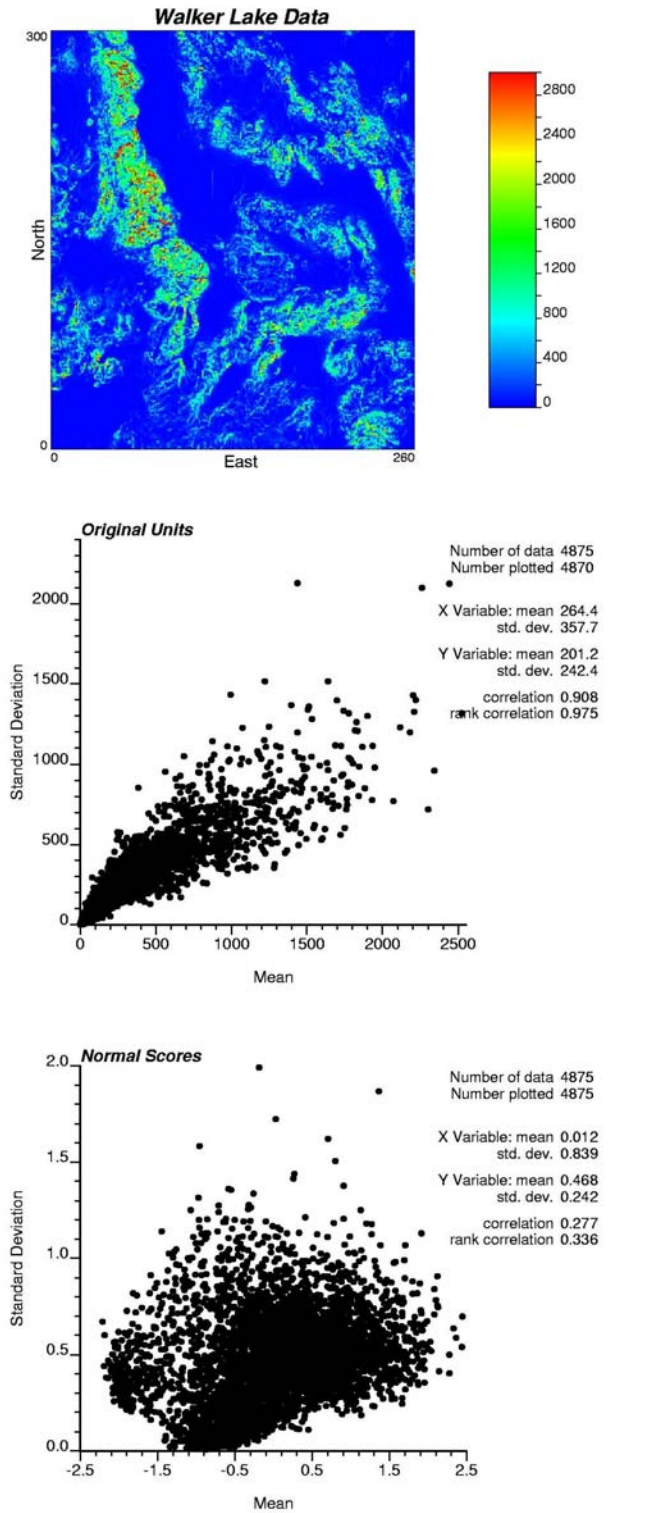


Figure 1: Color scale map of the Walker Lake data variable (top), the proportional effect of the original variable (middle), and the proportional effect of the normal scores variable (bottom). Note the strong proportional effect (relationship between standard deviation and mean) in original units and the weak proportional effect after normal scores transformation.

Figure 2: An illustration of the proportional effect for porosity data from a North Sea reservoir (top two figures) and for permeability from the same reservoir. Note the strong proportional effect for both porosity and permeability. Note also how this proportional effect disappears after normal scores transformation.

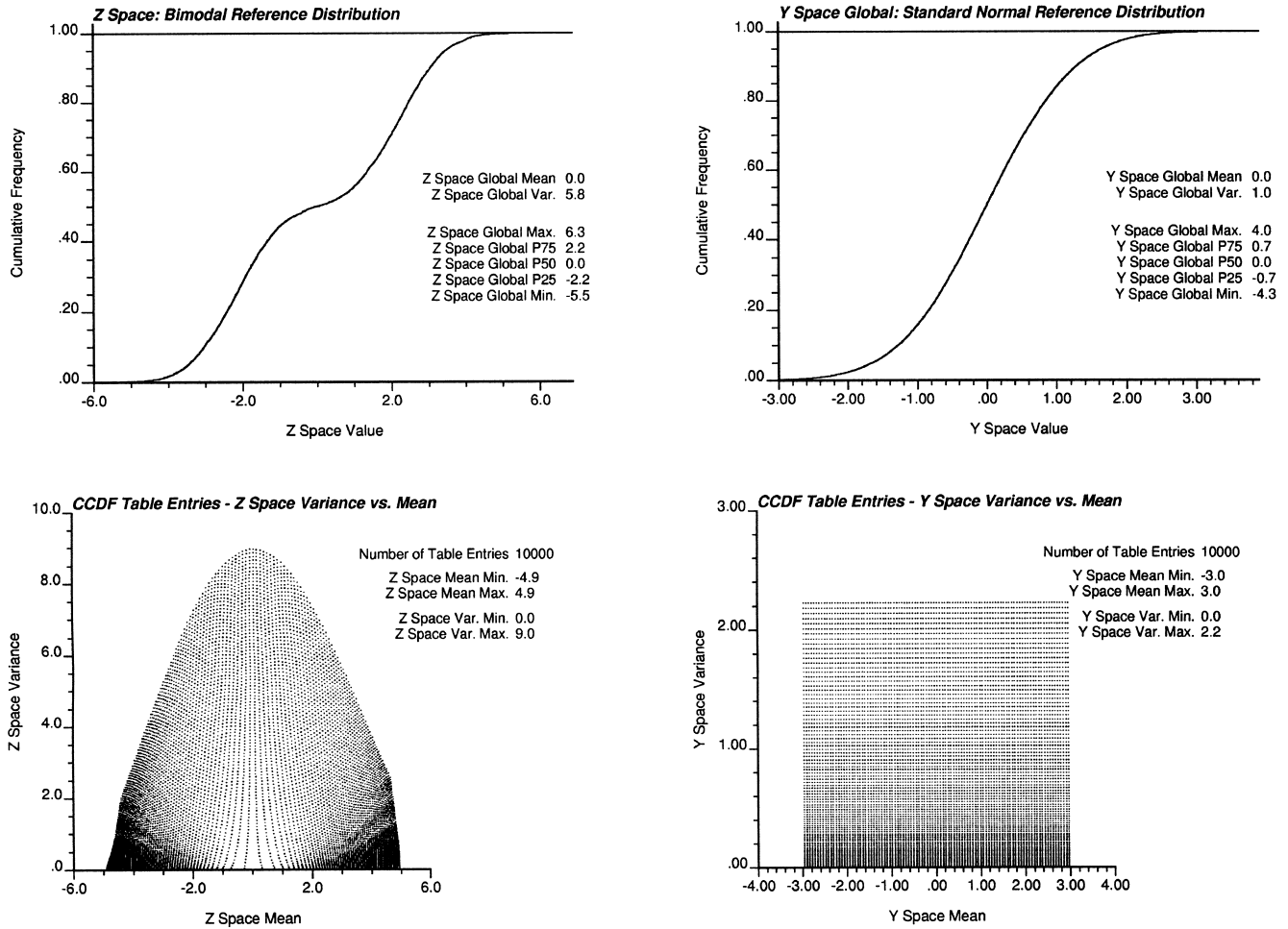


Figure 3: An illustration of the construction of the local distribution look up table. The Z space reference distribution is set as a bimodal distribution (top left) while the Y space is the required standard normal distribution (top right). The regular series of means and variances, for which local distributions were calculated, are shown (lower right). The resulting means and variances of the Z space local distribution table entries are shown in the lower left.

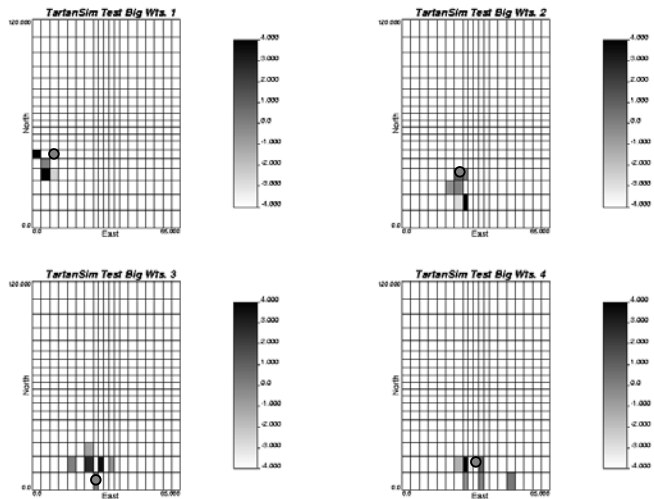


Figure 4: A variety of estimation settings that resulted in extreme weights. The estimation location coded with a weight of 0.0 and a grey dot and the conditioning data (previously simulated nodes) are coloured according to their weights.

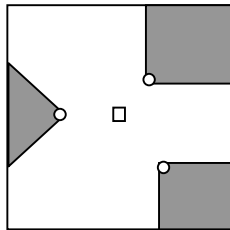


Figure 5: An example of the Boolean matrix that prevents screened data from being selected as conditioning data. This is a 2D example where three data have already been chosen as conditioning (circles). The shadow templates (grey areas) are located with their apexes on the accepted conditioning data and radiate away from the location being estimated (square at center).

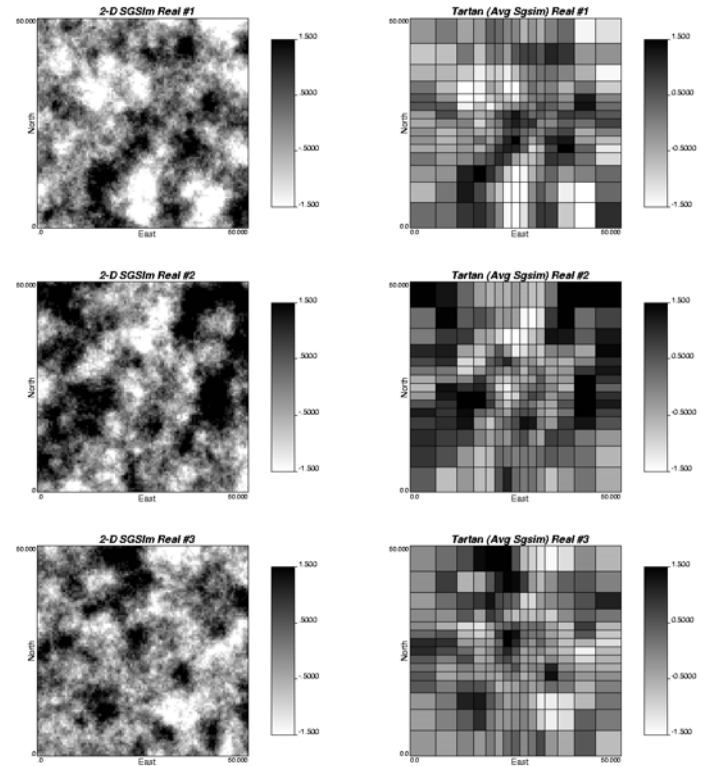


Figure 6: Example unconditional SGSIM realizations and the associated block averaged results.

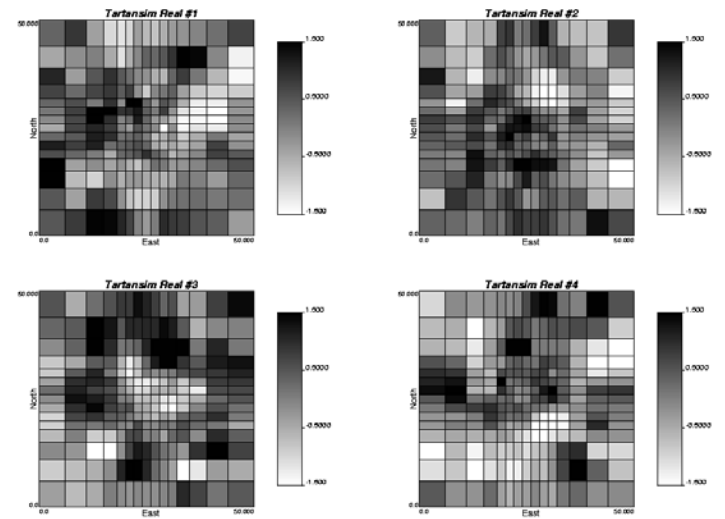


Figure 7: Example unconditional TARTANSIM realizations.

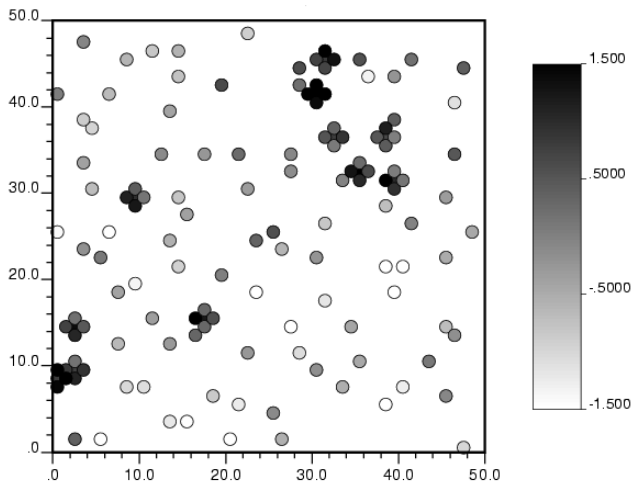


Figure 8: GSLIB data locations for conditional simulation.

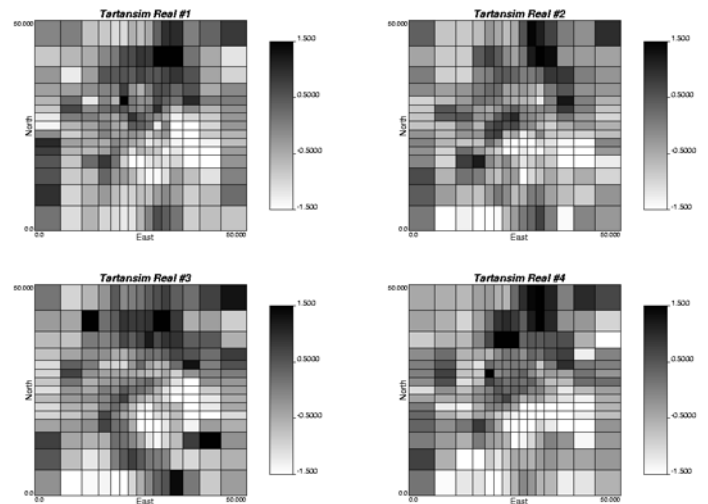


Figure 10: Example conditional TARTANSIM realizations.

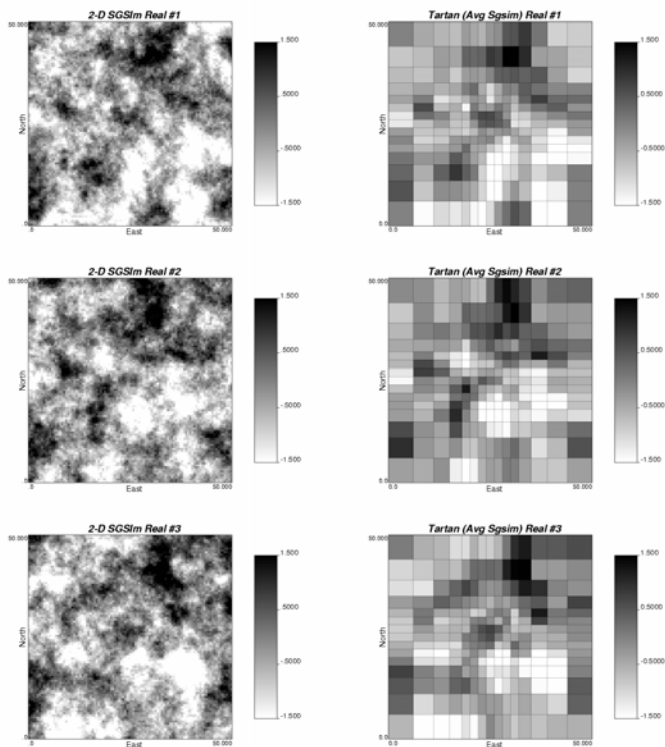


Figure 9: Example conditional SGSIM realizations and the associated block averaged maps.

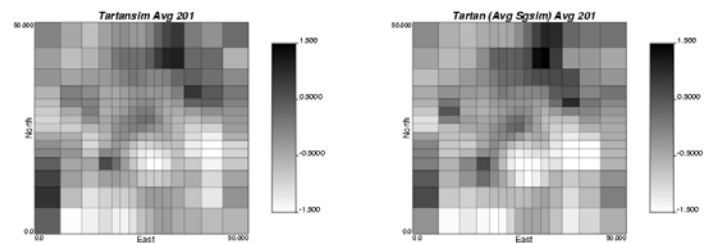


Figure 11: The e-type estimates over 201 realizations for both TARTANSIM and block averaged SGSIM.

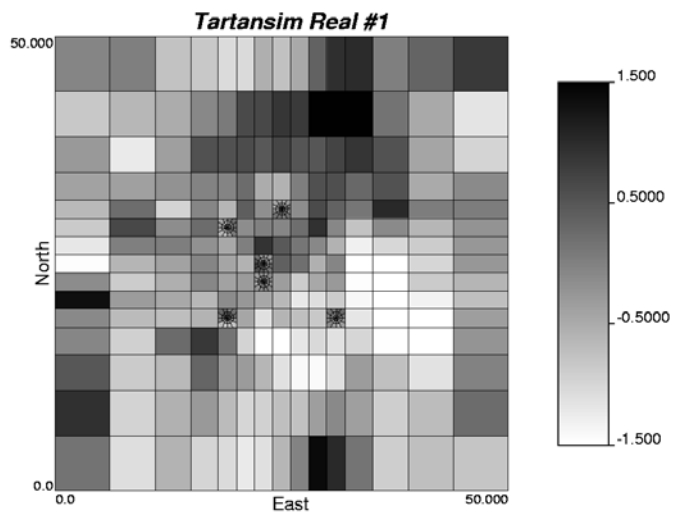


Figure 12: A TARTANSIM realization with six embedded radial grid simulations.

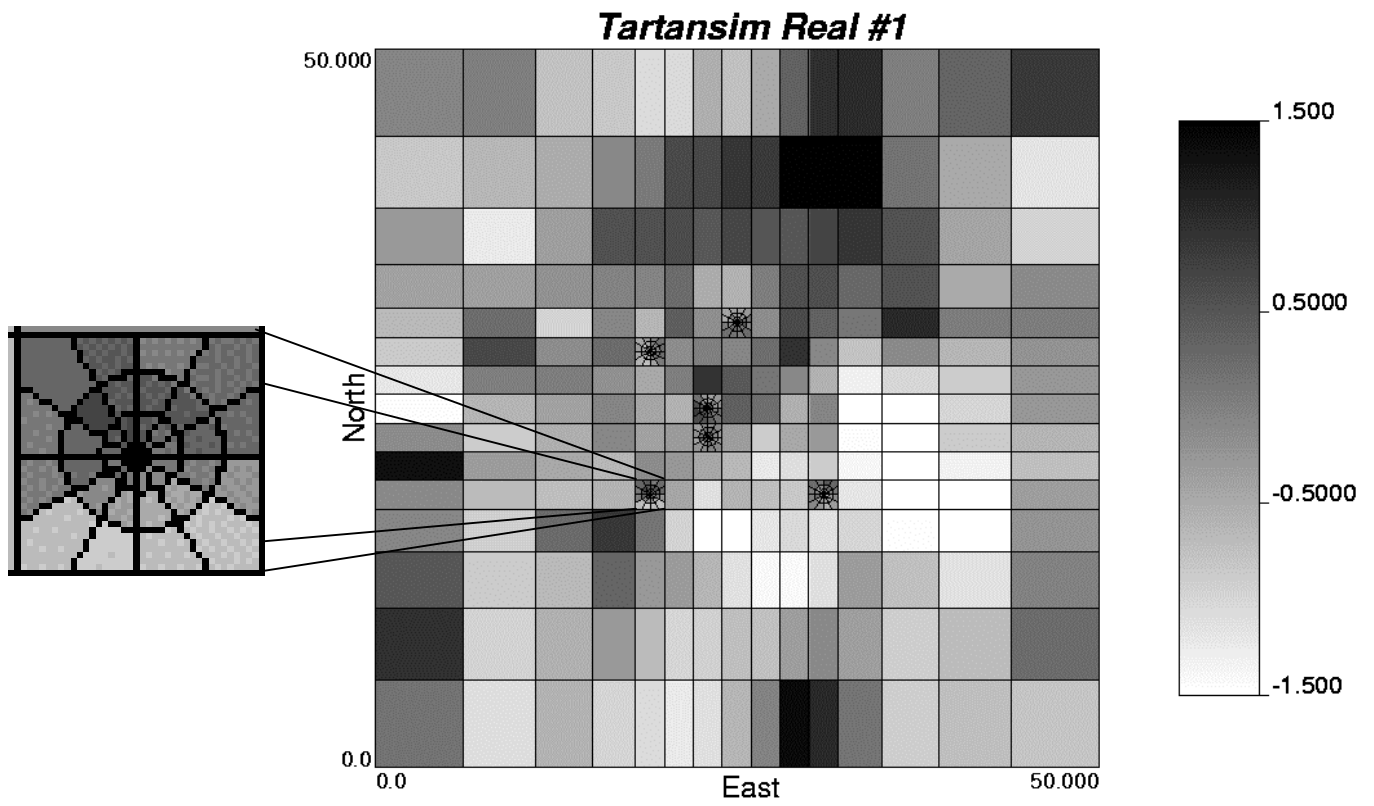


Figure 13: An example of a nested radial grid.